CHIN. PHYS. LETT. Vol. 34, No. 10 (2017) 104202

The 8 × 10 GHz Receiver Optical Subassembly Based on Silica Hybrid Integration Technology for Data Center Interconnection *

Chao-Yi Li(李超懿)[1,2], Jun-Ming An(安俊明)[1,2**], Jiu-Qi Wang(王九琦)[3], Liang-Liang Wang(王亮亮)[1], Jia-Shun Zhang(张家顺)[1], Jian-Guang Li(李建光)[1], Yuan-Da Wu(吴远大)[1,2], Yue Wang(王玥)[1], Xiao-Jie Yin(尹小杰)[1], Yong Li(李勇)[4], Fei Zhong(钟飞)[4]

[1] *State Key Laboratory on Integrated Optoelectronics, Institute of Semiconductors, Chinese Academy of Sciences, Beijing 100083*

[2] *College of Material Science and Optoelectronic Technology, University of Chinese Academy of Sciences, Beijing 100049*

[3] *College of Software, Beihang University, Beijing 100191*

[4] *Henan Shi Jia Photons Technology Co., Ltd, Hebi 458030*

(Received 25 July 2017)

An 8×10 GHz receiver optical sub-assembly (ROSA) consisting of an 8-channel arrayed waveguide grating (AWG) and an 8-channel PIN photodetector (PD) array is designed and fabricated based on silica hybrid integration technology. Multimode output waveguides in the silica AWG with 2% refractive index difference are used to obtain flat-top spectra. The output waveguide facet is polished to 45° bevel to change the light propagation direction into the mesa-type PIN PD, which simplifies the packaging process. The experimental results show that the single channel 1 dB bandwidth of AWG ranges from 2.12 nm to 3.06 nm, the ROSA responsivity ranges from 0.097 A/W to 0.158 A/W, and the 3 dB bandwidth is up to 11 GHz. It is promising to be applied in the eight-lane WDM transmission system in data center interconnection.

PACS: 42.79.Sz, 42.82.Fv, 42.82.Bq DOI: 10.1088/0256-307X/34/10/104202

With the rapid development of the big data, cloud computing and mobile communication, the data traffic has been growing exponentially.[1] IEEE specifies several standards to deal with the problem such as 802.3ba and 802.3bs.[2,3] They use the four or eight wavelengths division multiplexing (WDM) technology and high-order modulation format[4] to expand transmission capacity in transmitters and receivers. The key components are transmitter optical sub-assembly (TOSA) and receiver optical sub-assembly (ROSA) which consists of lasers, photodetectors (PDs) and (de)multiplexing components. There are several integration technologies to assemble them, including discrete integration, hybrid integration and monolithic integration. Discrete integrations use discrete components to realize photoelectric conversion,[5,6] which are time consuming and size inefficient. Monolithic integration is not mature, whose yield and volume are too small.[7,8] Therefore, the two methods are unsuitable for large-scale commercialization. Hybrid integration is the best and most accessible technology to be applied considering cost and size. At the receiving end, there are two main types of hybrid integration, one is using thin-film filters as demultiplexers[9] and the other one is using the PLC AWG as demultiplexers[10] in recent years. However, the lens and prism are used frequently to change the propagation of light or select specified wavelength, and it increases the assembly complexity and cost.[11,12]

In this work, we fabricate an 8 × 10 GHz ROSA with an 8-channel silica AWG as the demultiplexer and an 8-channel Ge/Si mesa-type PIN PD array based on the hybrid integrated technology. The output end facet of AWG is polished to 45° bevel to couple with a PD array rather than optical gratings[13] or 90° electrode structure surrounding PD array,[14] which simplifies the packaging process and reduces the cost. The ROSA is promising to be the key component in the transceivers applied in data center interconnection.

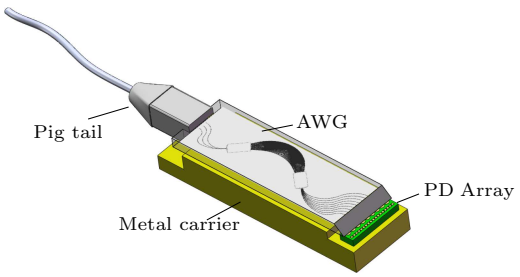

Fig. 1. Schematic diagram of the ROSA.

Figure 1 shows the structure of ROSA. It contains an 8 ch silica PLC AWG and an 8 ch PIN PD array with the 250 μm output waveguide spacing. The output end facet has been polished to 45° bevel to change the light-wave transferring from horizontal direction in the waveguide to vertical direction. Then, the light can be collected by the Ge/Si mesa-type PIN PD array through photosensitive surface. The AWG and

*Supported by the National High Technology Research and Development Program of China under Grant No 2015AA016902, the National Natural Science Foundation of China under Grant Nos 61435013 and 61405188, and the K. C. Wong Education Foundation.

**Corresponding author. Email: junming@semi.ac.cn

© 2017 Chinese Physical Society and IOP Publishing Ltd

PD array are mounted on a metal carrier made of 80% tungsten and 20% copper coated with gold to obtain high thermal conductivity and electrical conductivity.

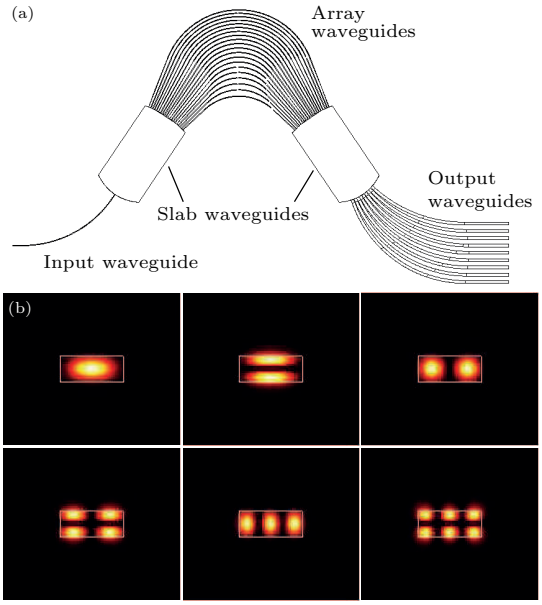

Fig. 2. (a) Schematic diagram of the AWG. (b) High-order modes with the 11 μm width of output waveguide.

A silica AWG is composed of input/output waveguides, input/output slab waveguides and array waveguides, as shown in Fig. 2(a). According to the actual process conditions and the chip size limitation, the silica material with 2% refractive index difference is chosen to reduce the coupling loss between input waveguides and optical fibers considering the spot size. The index of cladding waveguides and the core waveguides are 1.447 and 1.47653, respectively. To guarantee single mode transmission, the rectangular waveguide single mode conditions are used to determine the height and width of input/array waveguides and slab waveguide,[15]

$$m = \frac{2h}{\lambda_0}\sqrt{n_1^2 - n_2^2}, \tag{1}$$

$$b_{\max} = 2^{-\frac{3}{2}}\Delta^{-\frac{1}{2}}\frac{\lambda_0}{n_1}, \tag{2}$$

where m is the number of modes that can be integer, h is the height of waveguide, n_1 and n_2 are the refractive indexes of core and cladding waveguides, respectively, and $b_{\max}$ is max width of waveguide to maintain single mode. Moreover, the optical confinement factor was taken into consideration as well. As a result, the width and height of waveguides were both set as 4 μm.

The eight wavelengths of IEEE 802.3bs are specified as 1273.55, 1277.89, 1282.26, 1286.66, 1295.56, 1300.05, 1304.58 and 1309.14 nm, respectively. The channel spacing between the fourth channel and fifth channel is twice the others', thus the AWG has 9 channels actually whose center channel is ignored to follow the specification. Then other parameters including the length difference between the adjacent array waveguides ΔL and the diameter of the Rowland circle R are determined by the regular process.[16,17]

Because the single-mode laser cannot obtain absolute single wavelength and has slight linewidth inevitably, the flat-top responsivity spectrum to make full use of all the optical power is expected. Thus the multimode waveguide is chosen instead of the regular single-mode waveguide as the output waveguide.[18] The multimode waveguide can stimulate high-order modes, as seen in Fig. 2(b). Different modes overlap to form a box-like spectrum and can also increase the receiving tolerance ranges. By changing and optimizing the width of output waveguide, the output waveguide size is determined to 4 μm × 11 μm[19] and the whole AWG chip size is 11 mm × 4 mm ultimately. The detailed parameters are listed in Table 1.

Table 1. AWG parameters.

Name	Symbol	Value
Center wavelength (μm)	λ	1.2911
Frequency spacing (GHz)	Δf	800
Waveguide thickness (μm)	h	4
Array waveguide width (μm)	a	4
Output waveguide width (μm)	b	11
Array waveguide spacing (μm)	d	8
Output waveguide spacing (μm)	Δx	13
Adjacent array waveguide length difference (μm)	ΔL	20.243
Roland circle diameter (μm)	R	1465.2
Array waveguide number	M	59

The PD adopted is the Ge/Si mesa-type PIN PD, which is suitable for hybrid integration due to its high responsivity. The photosensitive surface diameter of PIN PD array is about 36 μm and the responsivity is up to 0.9 A/W. The bandwidth of Ge/Si PIN PD is mainly limited by the carrier transit time and the RC time constant, which are defined by [20]

$$f_{\text{transit}} = \frac{0.44 v_{\text{sat}}}{W}, \tag{3}$$

$$f_{\text{RC}} = \frac{1}{2\pi RC}, \tag{4}$$

where v_{sat} is the saturation drift velocity in Ge, W is the thickness of the intrinsic Ge film, R is a load resistance (e.g., 50 Ω), and C is the capacitance of the device. The 3 dB frequency of the device can be estimated by [20]

$$f_{3\text{dB}} = \sqrt{\frac{1}{1/f_{\text{transit}}^2 + 1/f_{\text{RC}}^2}}. \tag{5}$$

According to the above three formulas, the 3 dB bandwidth each channel is estimated 11.805 GHz theoretically under the conditions that v_{sat} is 6×10^6 cm/s, C is 0.16 pF, and W is about 1.8 μm.

The 45° of the output end facet of the AWG is simulated using finite-difference time-domain (FDTD) solutions under different propagation distances, as seen in Fig. 3. Figure 3(a) is the side view of the bevel, from which it can be seen that four 36 μm × 36 μm square

monitors are set parallel to the top facet of the AWG, and the distances between the four monitors and the facet are 0, 10, 20 and 30 μm, respectively. Figure 3(b) shows that light loss increases with extending the distance. The spot sizes were also demonstrated, which are perpendicular with waveguide at the end of AWG under different propagation distances, as seen in Fig. 4. With increasing the distance, the light fields expand correspondingly. If the propagation distance is too long, the PD array cannot collect all light power, which will cause extra loss. For example, the spot size is near 20 μm when the transmission distance is 30 μm. The active coupling is more difficult, because the tolerance is smaller and not all output light could enter into the PD array due to the fluctuation of channel spacing and coupling error in manual operation. In the actual coupling process, the longest distance between PD mesa and surface of AWG is less than 30 μm due to the step height of the metal carrier, thus the coupling efficiency is less than 2 dB theoretically according to the data from Fig. 3(b).

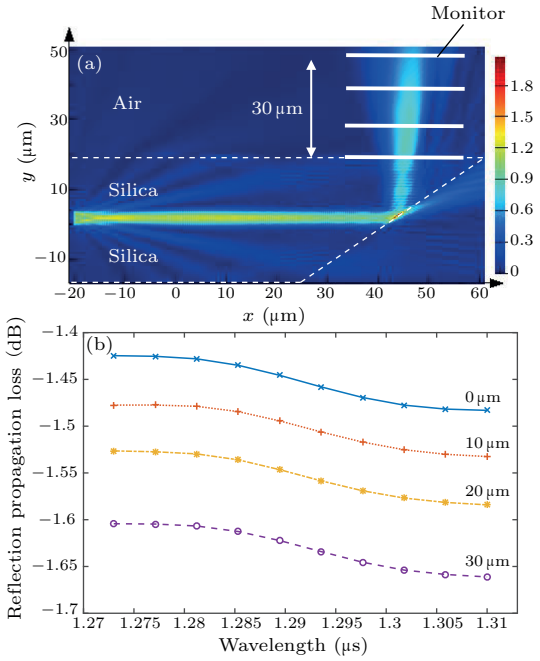

Fig. 3. (a) Longitudinal section of propagation simulation with angle of 45°. (b) Reflection propagation loss after 45° reflection under different propagation distances.

The AWG was fabricated by silica processing platform. Firstly, the core silica waveguides were deposited using PECVD with germanium doping. Then the input/output and array waveguides were etched using ICP etching. Lastly, the upper cladding silica was deposited using PECVD again. The fabrication process is shown in Fig. 5. The AWG performance without polishing bevel was tested and the results show that the insertion loss ranges from −3.3 dB to −4.3 dB of all 8 channels and the crosstalk between adjacent channel is less than −20 dB. The insertion loss of AWG can be improved by increasing the radius of the curved waveguide, which is the cost of compactness.

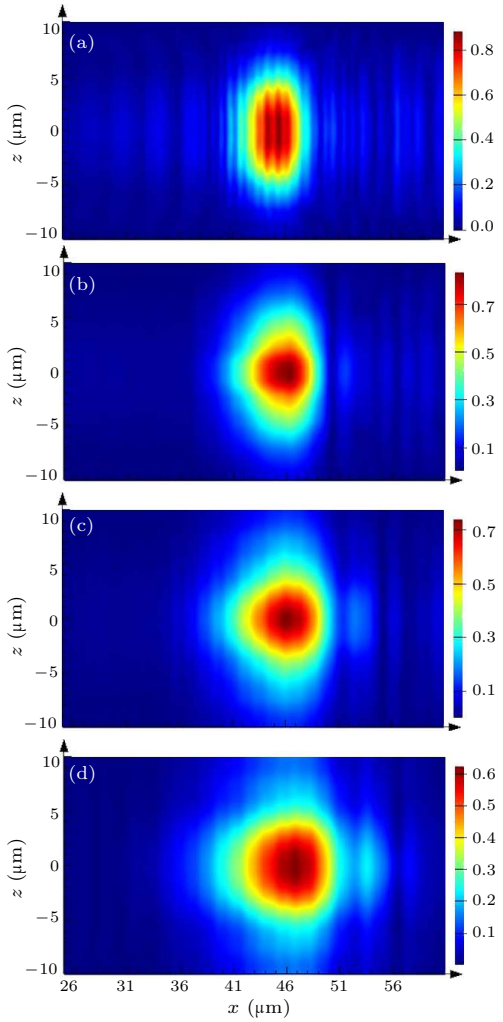

Fig. 4. Spot size diagram in 45° reflection under 0 (a), 10 (b), 20 (c) and 30 μm (d) propagation distance from the top side of AWG.

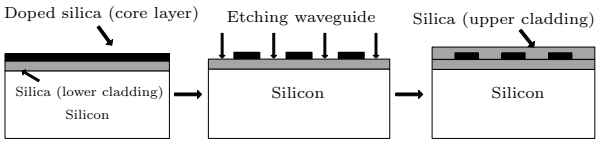

Fig. 5. Fabrication process of silica AWG.

The 45° bevel was made by three steps. Firstly, the AWG was fixed on the 45° lathe, and the iron grinding wheel was used to form 45° bevel roughly. Then the chip was polished on iron plate using SiC particles of 1 μm diameter for about 30 min. Lastly, 0.5 μm diameter CeO_2 particles were used to ultra-finely polish for about 30 min, making the bevel extremely smooth. During the process, it is highly necessary to pay attention to avoiding the crack of the AWG because of the stress.

The hybrid integration technology with active coupling process was used to assemble the AWG and PD array on the metal carrier. Firstly, the PD was fixed on the carrier using conductive adhesive by adjust-

ing the location of AWG with the input of O band ASE light source. Then, probes were used to detect the intensity of photocurrent of PD array as well as to provide bias voltage to PD. Finally, the AWG was fixed on the carrier by UV glue when the photocurrent comes to the maximum, as shown in Fig. 7.

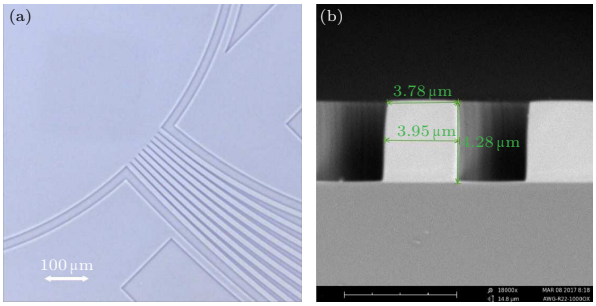

Fig. 6. (a) Photograph of top view of output waveguides. (b) Cross section of array waveguides.

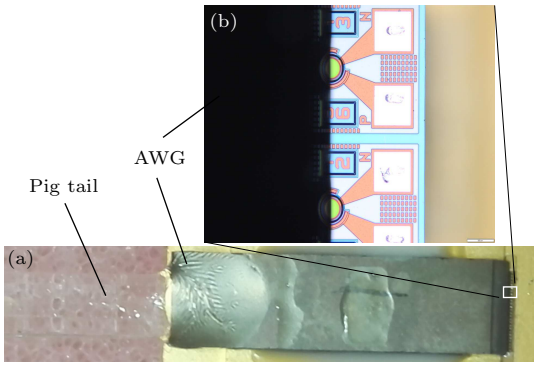

Fig. 7. (a) Photograph of the whole ROSA. (b) The partial magnification of ROSA.

The wavelength dependence of responsivity spectrum was measured, as shown in Fig. 8. A flat-top spectrum as expected design was obtained and the single channel 1 dB bandwidth ranges from 2.12 nm to 3.06 nm, which is close to the 2.8 nm 0.5 dB bandwidth of international level.[10] However, the performance of fifth and eighth channels is not very ideal. The insertion loss of the fifth channel is slightly higher than the other channels, which may be caused by the fabrication process. The deficiency of the eighth channel is that the spectrum of the channel is not as flat as that of the other channels. Because the bending radius of the 8th channel is so small, which is the smallest among 8 channels, high-order modes will dissipate when transmitting through the waveguide, and the spectrum is not flat for the lack of the mode quantity. The central wavelength of each channel is compliant with IEEE 802.3bs standard basically. The maximum responsivity of all 8 channels is about 0.158 A/W@−3 V, which means that it has about −7.5 dB loss in AWG chip and coupling process. AWG's insertion loss is slightly high because of the waveguides' small bending radius for compact size. However, the 45° bevel was used rather than lens and 90° electrode structure, thus the cost and the complexity of packaging are much lower. If the AWG's structure and the bevel's angle are further optimized, the performance of ROSA can be improved in the future. According to the above simulated and measured results, there is over −1 dB extra loss maybe due to the PD array responsivity non-uniformity and manual coupling error. Figure 9 shows the relation between the input light power and the photocurrent. It reveals high linearity up to at least 10 mW and we can meet the practical requirements of PAM-4 modulation format basically.

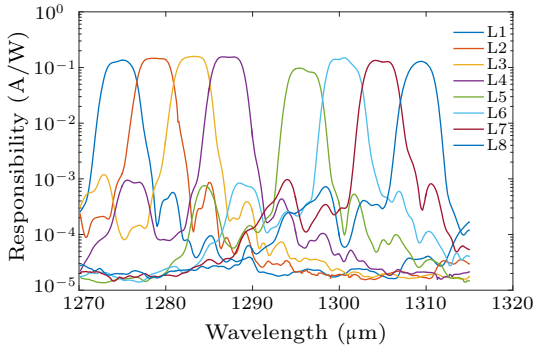

Fig. 8. Responsivity spectrum.

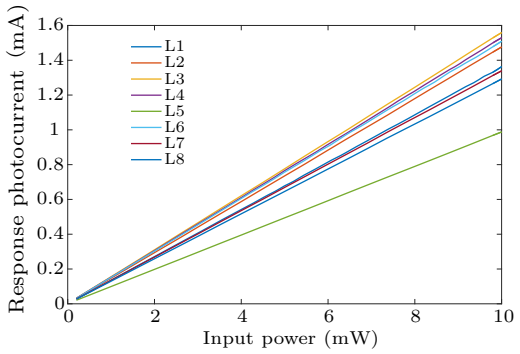

Fig. 9. Photocurrent-light power (I–P) relationship curve.

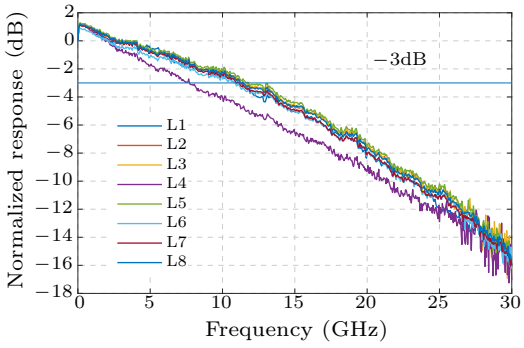

Fig. 10. Small-signal electro-optical response.

The small signal electro-optical frequency response was also measured, as seen in Fig. 10. The 3 dB bandwidth is over 11 GHz@−3 V except one channel, whose bandwidth is only up to 7 GHz. PD array has a certain rejection rate, thus the fifth PD does not work in good performance. The result verifies the above theory and

is equivalent to data rate of 28 Gb/s in PAM-4 format transmission.[21] The ROSA is promising for use in 200 G data center interconnection, which has reached the domestic level.[22] If the PD array is replaced by 50 Gb/s rate each channel, the ROSA can be applied in 400 G data center interconnection.

In conclusion, an 8-channel ROSA consisting of a silica AWG and a mesa-type PIN PD array has been designed and assembled. The total footprint is 12 mm × 5 mm × 2.5 mm including metal carrier. The 1 dB bandwidth of AWG ranges from 2.12 nm to 3.06 nm of all 8 channels. The maximum receiving responsivity is 0.158 A/W and the single channel 3 dB bandwidth of electro-optical frequency response is up to 11 GHz, which is promising to be applied in multi-wavelength high-speed transceivers in 400 G data center interconnection.

References

[1] Zhang L, Lu D, Li Z et al 2016 *J. Semicond.* **37** 124005
[2] IEEE P802.3bs 200Gb/s and 400Gb/s Ethernet Task Force. http://www.ieee802.org/3/bs/
[3] IEEE P802.3ba 40Gb/s and 100Gb/s Ethernet Task Force. http://www.ieee802.org/3/ba/
[4] Motaghiannezam R, Pham T, Chen A et al 2016 *Opt. Express* **24** 7374
[5] Arima R, Hatano T, Hiramoto K et al 2010 *Optical Fiber Communications Conference and Exhibition (Ofc)* (March 21–25 2010 San Diego, United States) p PDPD3
[6] Arima R, Yamashita T, Yahagi T et al 2011 *Optical Fiber Communications Conference and Exhibition (Ofc)* (March 6–10 2011 Los Angeles, United States) p JWA9
[7] Tolstikhin V, Wu F, Logvin Y et al 2013 *Optical Fiber Communications Conference and Exhibition (Ofc)* (March 17–31 2013 Anaheim, United States) p IW5A.4
[8] Ye H, Han Q, Lv Q Q et al 2017 *Chin. Opt. Lett.* **15** 082301
[9] Kawamura M, Nakajima F, Oomori H et al 2017 *Opt. Fiber Commun. Conf. Exhibition (Ofc)* (March 19–23 2017 Los Angeles, United States) p Th3B.2
[10] Doi Y, Nakanishi Y, Yoshimatsu T et al 2015 *Eur. Conf. Opt. Communication* (September 27–October 1 2015 Valencia, Spain) p 0097
[11] Nakajima F, Kawamura M, Oki K et al 2013 *Photon. Conf. (IPC)* (September 8–12 2013 Bellevue, United States) p TuG3.1
[12] Mochizuki K, Itamoto H, Aruga H et al *15th Optoelectronics, Communications Conference (OECC2010)* (July 5–9 2010 Sapporo Japan) p 7E3-2
[13] Xu H H, Hu Y T, Zhu Y et al 2010 *7th IEEE International Conference on Group IV Photonics* (September 1–3 2010 Beijing, China) p 126
[14] Ogawa I, Doi Y, Hashizume Y et al 2006 *IEEE J. Sel. Top. Quantum Electron.* **12** 1045
[15] Xu Y Q, Liang C G, Yang Y J et al 2001 *Chin. J. Semicond.* **22** 1546 (in Chinese)
[16] Yuan P, Wu Y D, Wang Y et al 2015 *J. Semicond.* **36** 084005
[17] Pan P, An J M, Wang H J et al 2014 *Chin. Phys.* B **23** 044210
[18] Amersfoort M R, Deboer C R, Vanham F P G M et al 1994 *Electron. Lett.* **30** 300
[19] Li C Y, An J M, Zhang J S et al 2107 *Acta Photonica Sin.* **46** 0823003 (in Chinese)
[20] Liu J F, Michel J, Giziewicz W et al 2005 *Appl. Phys. Lett.* **87** 103501
[21] Bhoja S 2017 *Opt. Fiber Commun. Conf. Exhibition (Ofc)* (March 19–23 2017 Los Angeles, United States) p W4D.5
[22] Lv Q Q, Pan P, Ye H et al 2016 *Chin. Phys.* B **25** 038505